Riemannian metrics on 2D manifolds related to the Euler-Poinsot rigid body problem

Bernard Bonnard, Olivier Cots, Nataliya Shcherbakova

▶ **To cite this version:**

Bernard Bonnard, Olivier Cots, Nataliya Shcherbakova. Riemannian metrics on 2D manifolds related to the Euler-Poinsot rigid body problem. 52nd IEEE Conference on Decision and Control (CDC 2013), Dec 2013, Firenze, Italy. pp. 1804-1809. hal-00925078v2

HAL Id: hal-00925078
https://hal.science/hal-00925078v2

Submitted on 23 Feb 2017

HAL is a multi-disciplinary open access archive for the deposit and dissemination of scientific research documents, whether they are published or not. The documents may come from teaching and research institutions in France or abroad, or from public or private research centers.

L'archive ouverte pluridisciplinaire **HAL**, est destinée au dépôt et à la diffusion de documents scientifiques de niveau recherche, publiés ou non, émanant des établissements d'enseignement et de recherche français ou étrangers, des laboratoires publics ou privés.

Open Archive TOULOUSE Archive Ouverte (OATAO)

OATAO is an open access repository that collects the work of Toulouse researchers and makes it freely available over the web where possible.

This is an author-deposited version published in : http://oatao.univ-toulouse.fr/
Eprints ID : 17149

The contribution was presented at CDC 2013 :
http://www.ieeecss.org/CAB/conferences/cdc2013/

To cite this version : Bonnard, Bernard and Cots, Olivier and Shcherbakova, Nataliya *Riemannian metrics on 2D manifolds related to the Euler-Poinsot rigid body problem.* (2014) In: 52nd IEEE Conference on Decision and Control (CDC 2013), 10 December 2013 - 13 December 2013 (Firenze, Italy).

Any correspondence concerning this service should be sent to the repository administrator: staff-oatao@listes-diff.inp-toulouse.fr

Riemannian metrics on 2D manifolds related to the Euler-Poinsot rigid body problem.

Bernard Bonnard, Olivier Cots and Nataliya Shcherbakova

***Abstract*— The Euler-Poinsot rigid body problem is a well known model of left-invariant metrics on $SO(3)$. In the present paper we discuss the properties of two related reduced 2D models: the sub-Riemanian metric of a system of three coupled spins and the Riemannian metric associated to the Euler-Poinsot problem via the Serret-Andoyer reduction. We explicitly construct Jacobi fields and explain the structure of conjugate loci in the Riemannian case and give the first numerical results for the spin dynamics case.**

I. INTRODUCTION

The Euler-Poinsot rigid body problem describes the motions of a rigid body fixed in its center of mass. It is one of the most famous problems in Classical Mechanics having many important applications, for instance, in attitude control of satellites in space engineering or in quantum systems.

The motions of the body are solutions to the Hamiltonian system associated to the Hamiltonian

$$H = \frac{1}{2}\left(\frac{H_1^2}{I_1} + \frac{H_2^2}{I_2} + \frac{H_3^2}{I_3}\right),$$

where I_i, $i = 1,2,3$ are the principal momenta of inertia, and H_i are the components of the angular momentum vector written in the moving frame that coincides with the principal axes of inertia of the body ([1]). This vector is related to the angular velocity vector (u_1,u_2,u_3) via the formula $H_i = u_i I_i$.

The system of equations of the Euler-Poinsot motion is Liouville integrable, and every trajectory is determined by the values of two first integrals: H and $G = \sum_{i=1}^{3} H_i^2$. Thus in the space of momenta H_i the motion of the body can be described by the curves of intersections of the energy ellipsoid $H = const$ with the sphere of angular momentum $G = const$ called *polhodes* in Classical Mechanics. Except the so-called separating polhodes, every trajectory evolves on a 2D torus, where the motion is pseudo-periodic with one frequency equal to zero.

From the optimal control point of view, the motions of the rigid body are the extremals of the following optimal control problem:

$$\dot{R}(t) = R(t)\begin{pmatrix} 0 & -u_3 & u_2 \\ u_3 & 0 & -u_1 \\ -u_2 & u_1 & 0 \end{pmatrix},\ \frac{1}{2}\int_0^T \sum_{i=1}^{3} u_i^2 I_i \to \min_{u(\cdot)},$$

B. Bonnard is with Institut de Mathématiques de Bourgogne, Université de Bourgogne, 9 avenue Alain Savary, 21078 Dijon, France, Bernard.Bonnard@u-bourgogne.fr

O. Cots is with INRIA Sophia Antipolis Méditerranée, 06902 Sophia Antipolis, France, olivier.cots@inria.fr

N. Shcherbakova is with Université de Toulouse, INPT, UPS, Laboratoire de Génie Chimique, 4 allée Emile Monso, 31432 Toulouse, France, nshcherb@inp-toulouse.fr

which provides a model of a left-invariant Riemanian metric on $SO(3)$ ([6]). Here $R(t) \in SO(3)$ is the matrix of directional cosines describing rotations of the moving frame with respect to some inertial frame, and $T > 0$ is fixed. In the optimal control context, one of the most important tasks is the calculation of conjugate and cut loci of the trajectories, i.e., the sets in the state space where the extremals stop to be optimal (in the local or in the global sense). Computing these sets is equivalent to solving the Hamilton-Jacobi-Bellman equation, and in general it is a very difficult mathematical problem. In this paper we consider two particular models, where the dynamics of the system can be reduced to a 2D manifold: the problem of three spin-$1/2$ particles, which leads to an almost- Riemannian metric on S^2, and the metric related to the Serret-Andoyer reduction.

The Serret-Andoyer reduction allows to integrate the Euler Poinsot problem by using a set of appropriate symplectic variables ([4], [8]). The new 2D problem defines a Riemmanian metric in the factor space, which admits the polar form $ds^2 = d\varphi^2 + m(\varphi)d\theta^2$. In Sections II we describe the properties of this reduction and of the associated Riemannian metric. The conjugate times can be computed explicitly due to the integrability property. On the other hand, using the polar form of the metric we explicitly construct the Jacobi fields and obtain an exhaustive description of the conjugate locus.

In Section III, we present our numerical results concerning the cut and conjugate loci of the spin problem using the HamPath code. This 2D model can be seen as the limit case of the original Euler-Poinsot problem when $I_2 \to \infty$, or as a deformation of the well known Grushin metric. We consider our results as the first step toward the computation of the conjugate locus in the full 3D Euler-Poinsot problem.

II. THE SERRET-ANDOYER REDUCTION OF THE EULER-POINSOT PROBLEM

A. The Serret-Andoyer canonical variables

The Serret-Andoyer variables x, y, w, p_x, p_y, p_w, where p_x, p_y, p_w denote canonical impulses associated to x, y, and w, are defined by $H_1 = \sqrt{p_x^2 - p_y^2}\sin y$, $H_2 = \sqrt{p_x^2 - p_y^2}\cos y$ and $H_3 = p_y$. So, $|p_x| = \sqrt{G}$ and the Hamiltonian H takes the form

$$H_a = \frac{1}{2}\left((p_x^2 - p_y^2)(A\sin^2 y + B\cos^2 y) + Cp_y^2\right), \qquad (1)$$

where $y = \arctan(\frac{H_1}{H_2})$, $A = I_1^{-1}$, $B = I_2^{-1}$ and $C = I_3^{-1}$. A further canonical transformation is needed to get the standard action-angle representation ([7]). Instead, in this paper we

use the Serret-Andoyer reduction to transform the Euler-Poinsot problem into a 2D Riemmanian problem. Denoting $z(y) = 2(A\sin^2 y + B\cos^2 y)$, H_a takes the form

$$H_a = \frac{1}{2}\left(\frac{z(y)}{2}p_x^2 + \left(C - \frac{z(y)}{2}\right)p_y^2\right). \tag{2}$$

Observe that if the momenta of inertia of the body are ordered as $A < B < C$, then $z(y) \in [2A, 2B]$ and $2C - z(y) > 0$, therefore H_a is positive and it defines the Riemannian metric

$$g_a = z(y)^{-1}dx^2 + (2C - z(y))^{-1}dy^2, \tag{3}$$

which is referred as *the Serret-Andoyer metric* in the sequel.

Since H_a does not depend on w, $p_w = const$ is a first integral associated to the cyclic variable w. The reduced dynamics on the (x,y) plane is described by the Hamiltonian equations

$$\begin{aligned} \dot{x} &= p_x(A\sin^2 y + B\cos^2 y), \qquad \dot{p}_x = 0, \\ \dot{y} &= p_y(C - A\sin^2 y - B\cos^2 y), \\ \dot{p}_y &= (B-A)(p_x^2 - p_y^2)\sin y\cos y, \end{aligned} \tag{4}$$

where x is another cyclic variable and p_x is a first integral. Note that the dynamics on the plane (y, p_y) is described by a standard pendulum-type phase portrait. Indeed, H_a is π-periodic with respect to y, it verifies the symmetry relations:

$$H_a(y,p_y) = H_a(y,-p_y), \quad H_a(y,p_y) = H_a(-y,p_y), \tag{5}$$

and $p_y = 0$, $y = \frac{k\pi}{2}$, $k = 0,1$ are its points of equilibrium. A standard computation shows that the equilibrium $y = 0$, $p_y = 0$ is a saddle, while $y = \frac{\pi}{2}$, $p_y = 0$ is a stable equilibrium of center type. In particular, it follows that in order to parametrize all phase trajectories on the (y,p_y)-plane it would be sufficient to consider trajectories starting at $y(0) = \frac{\pi}{2}$. We summarize our analysis in the following:

Proposition 1. *The pendulum motion in the (y,p_y) plane can be interpreted on the cylinder $y \in [0,\pi] \bmod \pi$ with the stable equilibrium at $y = \frac{\pi}{2}$ and unstable ones at $y = 0,\pi$. There are two types of periodic trajectories on the cylinder: oscillating trajectories homotopic to zero, and rotating trajectories, while non-periodic trajectories are separatrices joining 0 to π, which correspond to separating polhodes of the full problem. Moreover, all these trajectories share the reflection symmetry with respect to the axes $y = 0$ and $p_y = 0$.*

B. Polar representation of the Serret-Andoyer metric

In what follows we assume that the principal momenta of inertia verify $A < B < C$. In order to obtain the Darboux normal form $g_a = d\varphi^2 + \mu(\varphi)d\theta^2$ for the metric (3), we must solve the pair of equations

$$\frac{dy}{\sqrt{C - (A\sin^2 y + B\cos^2 y)}} = d\varphi, \qquad d\theta = dx.$$

The second equation implies that $\theta = x$ modulo a rotation by a fixed angle x, so that in the sequel we assume $x \equiv \theta$. As for φ, according to Section II, we set $y_0 = \frac{\pi}{2}$. Let $\zeta = \sin y$, then $\zeta(0) = 1$ and

$$\int_{\varphi_0}^{\varphi} d\varphi = -\int_{\zeta}^{1} \frac{d\zeta}{\sqrt{(C-A)(1-\zeta^2)(k' + k\zeta^2)}},$$

where

$$k = \frac{(B-A)}{(C-A)}, \quad k' = 1 - k = \frac{(C-B)}{(C-A)}.$$

Denoting $\alpha = \sqrt{C-A}$ and choosing $\varphi_0 = 0$, we finally obtain a standard elliptic integral

$$-\alpha\varphi = \int_{\zeta}^{1} \frac{d\zeta}{\sqrt{(1-\zeta^2)(k' + k\zeta^2)}} = \mathrm{cn}^{-1}(\zeta|k).$$

Thus $\sin y = \zeta = \mathrm{cn}(-\alpha\varphi|k) = \mathrm{cn}(\alpha\varphi|k)$, which implies $z = 2(A\sin^2 y + B\cos^2 y) = 2(A\mathrm{cn}^2(\alpha\varphi|k) + B\mathrm{sn}^2(\alpha\varphi|k))$. So, we can now formulate the following

Proposition 2. *The Serret-Andoyer metric g_a can be put into the Darboux normal form $d\varphi^2 + m(\varphi)d\theta^2$ with $m(\varphi) = (A\mathrm{cn}^2(\alpha\varphi|k) + B\mathrm{sn}^2(\alpha\varphi|k))^{-1} \in [I_2, I_1]$, $\alpha = \sqrt{C-A}$ and $k = \frac{(B-A)}{(C-A)}$;*

In what follows $'$ denotes the derivative w.r.t. φ. The standard Gauss curvature formulae for Darboux-type metrics $G(\varphi) = -(\sqrt{m(\varphi)})''m(\varphi)^{-1/2}$ implies

Corollary 1. *The Gauss curvature of g_a is given by*

$$G(\varphi) = \frac{(A+B+C)(z(\varphi) - z_-)(z(\varphi) - z_+)}{z(\varphi)^2},$$

where $z(\varphi) = 2(A\mathrm{cn}^2(\alpha\varphi|k) + B\mathrm{sn}^2(\alpha\varphi|k))$ and

$$z_\pm = 2\,\frac{AB+AC+BC \pm \sqrt{(AB+AC+BC)^2 - 3ABC(A+B+C)}}{A+B+C}.$$

In particular, G is $\frac{2K(k)}{\alpha}$-periodic and reflectionally symmetric: $G(\varphi) = G(-\varphi)$. In addition, $z_- \in [2A, 2B]$, while $z_+ > 2B$, thus on $[-\frac{K(k)}{\alpha}, \frac{K(k)}{\alpha}]$ the Gauss curvature change it sign twice at $\pm\varphi_1$, $\varphi_1 = \alpha^{-1}\mathrm{sn}^{-1}(\sqrt{\frac{z_- - 2A}{2(B-A)}})$. It has local maxima at $\varphi = \pm\frac{K(k)}{\alpha}$ and $\varphi = 0$, and a minimum at the point φ_* such that $z(\varphi_*) = \frac{2z_-z_+}{z_- + z_+}$. More precisely,

$$\max_{[0,\frac{2}{\alpha}K(k)]} G(\varphi) = G(0) = \frac{(B-A)(C-A)}{A},$$

$$\min_{[0,\frac{2}{\alpha}K(k)]} G(\varphi) = -\frac{(A+B+C)(z_+z_-)^2}{4z_-z_+}.$$

These results are illustrated in Fig.1.

C. Jacobi fields for Riemannian metrics on 2D surfaces of revolution

In this section, using the Hamiltonian formalism, we construct the Jacobi fields for the Darboux-type metrics. As a by-product, we obtain the conjugate points equation.

Taking a local chart in an open domain U, the Riemannian metric on a two-dimensional surface of revolution can be written in polar coordinates in the form $g = d\varphi^2 + m(\varphi)d\theta^2$ where $m(\varphi) > 0$. Let $q = (\varphi,\theta) \in U$ denote the state

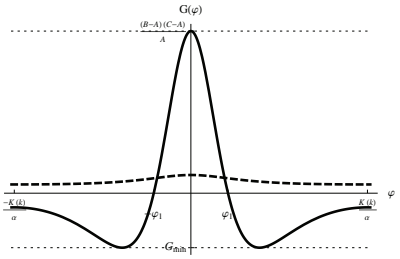

Fig. 1. The function $\mu(\varphi)$ (dashed curve) and Gauss curvature (continuous curve) of the Serret-Andoyer metric

variables and $p=(p_\varphi,p_\theta)$ the corresponding coordinates on fibers. At each point $z=(p,q)\in T^*U$ we denote by ∂_p and ∂_q the vertical and the horizontal parts of the linear space $T_z(T^*U)$. The Hamiltonian associated to g reads

$$H=\frac{1}{2}\left(p_\varphi^2+p_\theta^2\mu(\varphi)\right),\ \text{where}\ \mu(\varphi)=\frac{1}{m(\varphi)},$$

and the geodesics are projections on U of the extremal curves - solutions to the Hamiltonian system

$$\dot\varphi=p_\varphi,\quad \dot p_\varphi=-\frac{1}{2}p_\theta^2\mu'(\varphi),\quad \dot\theta=p_\theta\mu(\varphi),\quad \dot p_\theta=0,\ (6)$$

where p_θ is the first integral: $p_\theta=const$. System (6) admits two particular types of solutions: meridian curves with $p_\theta=0$ and $\theta(t)=\theta_0$, and parallel solutions characterized by $\dot\varphi(0)=p_\varphi(0)=0$ and $\varphi(t)=\varphi_0$, which, by (6), is equivalent to $\mu'(0)=0$.

In what follows we assume that

(A_1) $\varphi=0$ is a parallel solution (i.e. $\mu'(0)=0$);
(A_2) $\mu(\varphi)=\mu(-\varphi)$, and $\mu''(0)>0$.

Then on every energy level set $H=h>0$ in a neighborhood of $\varphi=0$ there is a family of periodic solutions to the equation $\dot\varphi^2=2h-p_\theta^2\mu(\varphi)$ describing the evolution of $\varphi(\cdot)$ along geodesics. Note that $\varphi(t)\in[-\bar\varphi,\bar\varphi]$, where $\bar\varphi:\ p_\theta^2\mu(\bar\varphi)=2h$.

The Hamiltonian function H defines a quadratic form on the cotangent bundle T^*U, we denote by $\vec H$ the associated Hamiltonian vector field and by $e^{t\vec H}$ the Hamiltonian flow generated by $\vec H$.

Definition 1. Let $t\to\gamma(t)$, $t\in[0,T]$, be a solution of (6). The variational system associated to (6) along $\gamma(\cdot)$ is called *the Jacobi equation*. The *Jacobi field* $J:\ [0,T]\to T_{\gamma(\cdot)}(T^*U)$ is a non-trivial solution of the Jacobi equation $J(t)=e_*^{t\vec H}J(0)$.

In practice, the computation of Jacobi fields reduces to the integration of the linearized Hamiltonian system $\dot w(t)=\frac{\partial H(\gamma(t))}{\partial z}w(t)$, where $w=\delta z$. Setting $w_1=\delta p_\varphi$, $w_2=\delta p_\theta$, $w_3=\delta\varphi$ and $w_4=\delta\theta$ from (6) we get

$$\dot w_1=-p_\theta\mu'(\varphi)w_2-\frac{p_\theta^2\mu''(\varphi)}{2}w_3,\quad \dot w_2=0,\qquad (7)$$
$$\dot w_3=w_1,\quad \dot w_4=\mu(\varphi)w_2+p_\theta\mu'(\varphi)w_3.$$

It follows that $w_2=const$, and moreover, (7) reduces to the second order equation

$$\ddot w_3+\frac{p_\theta^2\mu''(\varphi)}{2}w_3=-p_\theta\mu'(\varphi)w_2,\qquad (8)$$

where $\varphi=\varphi(t)$ is a known function along $\gamma(t)$, while p_θ and w_2 are constant. Once $w_3(t)$ is found, we immediately get $w_1=\dot w_3$, and $w_4(t)=w_4(0)+\int_0^t\left(w_2\mu(\varphi(\tau))+p_\theta\mu'(\varphi(\tau))w_3(\tau)\right)d\tau$.

D. Solving equation (8).

Let us rewrite (8) in the form $\ddot x+\Phi(t)x=\Psi(t)$, where $x=w_3$, $\Phi(t)=\frac{1}{2}p_\theta^2\mu''(\varphi(t))$, and $\Psi(t)=-p_\theta\mu'(\varphi(t))w_2$. This equation can be integrated in a rather standard way if we know a solution to the homogeneous equation $\ddot w(t)+\Phi(t)w(t)=0$. In our case, in view of (6), $w(t)=p_\varphi(t)$ satisfies this condition. Then (8) can be solved via the following procedure:

Step 1. Let y be such shat $x=wy$, and denote $\xi=\dot y$. Then

$$\dot\xi+a(t)\xi=b(t),\quad a(t)=\frac{2\dot w(t)}{w(t)},\quad b(t)=\frac{G(t)}{w(t)}$$

for all t such that $w(t)\neq0$. Denote $M(t)=\exp\left(\int_0^t a(\tau)d\tau\right)$. Then $(x(t)M(t))^{\cdot}=b(t)M(t)$, which yields $\xi(t)-\xi(0)=M(t)^{-1}\int_0^t b(\tau)M(\tau)d\tau$ provided $M(0)=1$.

Step 2. Taking $w(t)=p_\varphi(t)$ and using the definitions of Φ and Ψ, we get

$$a(t)=-\frac{p_\theta^2\mu'(\varphi(t))}{p_\varphi(t)},\quad M(t)=\frac{p_\varphi^2(t)}{p_\varphi^2(0)},$$

and hence

$$\xi(t)=\frac{p_\varphi^2(0)}{p_\varphi^2(t)}\left(-\frac{p_\theta w_2}{p_\varphi^2(0)}\left(\mu(\varphi(t))-\mu(\varphi_0)\right)+\xi(0)\right).\quad (9)$$

The final expression for $y(t)$ can be now computed via the quadrature: $y(t)=y(0)+\int_0^t\xi(\tau)d\tau$.

The whole basis of Jacobi vector fields can be now written by varying the initial conditions $w_i(0)$, $i=1\dots4$. Observe that the first three Jacobi fields can be easily recovered from the well known properties of the Hamiltonian systems associated to Riemannian metrics. Indeed, (8) admits two obvious solutions with $w_2=0$: the Hamiltonian vector fields $J_1=\vec H$ and $J_2=\vec p_\theta=\partial_\theta$, which are both invariant with respect to the tangent flow $e_*^{t\vec H}$. These two fields emanate from the horizontal part of the basis at $t=0$.

The remaining two fields can be obtained by taking vertical initial conditions $w_3(0)=w_4(0)=0$, $w_2\neq0$. Observe that if $p_\varphi(0)\neq0$ and $w_1(0)\neq0$, then $\xi(0)\neq0$. Setting $\xi(0)=1$ and $w_2=p_\theta$ is equivalent to take the Euler field $\vec E=p_\varphi\partial_\varphi+p_\theta\partial_\theta$ as the generator of the solution. Since $[\vec H,\vec E]=-\vec H$, and all Lie brackets of higher order are zero, we get $J_3(t)=\vec E+t\vec H$.

The computation of the only non-trivial Jacobi field $J_4(t)$ can be simplified by an appropriate choice of $\xi(0)$. For instance, we can take $y(0)=0$ and $\dot y(0)=\xi(0)=-\frac{p_\theta w_2\mu(\varphi_0)}{p_\varphi^2(0)}$. Then, setting $w_2=1$, taking into account that $w_3=p_\varphi y$ and $w_1=\dot w_3$, after all necessary simplifications, we get

$$w_3(t)=-p_\theta p_\varphi(t)\Lambda(\varphi(t)),\quad w_4=p_\varphi^2(t)\Lambda(\varphi(t)),$$

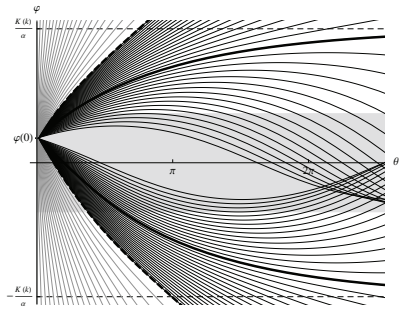

Fig. 2. Extremal curves of the Serret-Andoyer metric

$$w_1(t) = \frac{p_\theta^3 \mu'(\varphi(t))}{2}\Lambda(\varphi(t)) - \frac{p_\theta \mu(\varphi(t))}{p_\varphi(t)},$$

where

$$\Lambda(\varphi) = \int_{\varphi_0}^{\varphi} \frac{\mu(\bar\varphi)}{p_\varphi^3(\bar\varphi)} d\bar\varphi, \quad p_\varphi(\varphi) = \sqrt{2h - p_\theta^2 \mu(\varphi)}.$$

Remark 1. Though the above computation is valid under the assumption $w(t) = p_\varphi(t) \neq 0$ (see Step 1), $J_4(t)$ can be continuously extended to $\tilde t$ such that $p_\varphi(\tilde t) = 0$ (and hence $\mu(\varphi(\tilde t)) = 2hp_\theta^{-2}$). Indeed, some additional work yields

$$\Lambda(\varphi(t)) = \frac{K_0(t)}{p_\varphi(t)} - \frac{K_0(0)}{p_\varphi(0)} + K_1(t), \quad K_0(t) = \frac{2\mu(\varphi(t))}{p_\theta^2 \mu'(\varphi(t))} \tag{10}$$

where the function $K_1(t)$ is bounded as $t \to \tilde t$.

We resume our computation in the following

Proposition 3. *The vector fields J_1, J_2, $J_3(t)$ and $J_4(t)$ form a basis of Jacobi fields along a given solution $(\varphi(t), \theta(t), p_\varphi(t), p_\theta)$ of (6).*

Corollary 2. *Consider a Darboux type metric g verifying (A1), (A2). Then the conjugate (to 0) times along any periodic trajectory issued from the point (θ_0, φ_0) with $p_\varphi(0) \neq 0$ are solutions to the equation*

$$\Lambda(\varphi(t)) = 0. \tag{11}$$

The points $(\theta, \pm\bar\phi)$, where $\pm\bar\phi$ are the extremities of the variation of φ, are conjugate to each other.

Proof. By definition, the time t_* is said conjugate to $t_0 = 0$ if the differential of the end-point mapping $E^t_{q_0} : p(0) \mapsto q(t)$ degenerates at $t = t_*$. Written in terms of Jacobi fields, this definition is equivalent to the following condition:

$$\Delta_{t_*} = \det(J_3(0), J_4(0), J_3(t_*), J_4(t_*)) = 0.$$

Computing, we get $\Delta_t = 2ht\, p_\varphi(t)\Lambda(\varphi(t))$. Then, by (10), the conjugate time is a solution to $\Lambda(\varphi(t)) = 0$ for trajectories with $p_\varphi(0) \neq 0$. On the other hand, any periodic trajectory starting at $(\theta_0, \pm\bar\phi)$ has $p_\varphi(0) = p_\varphi(\frac{T}{2}) = 0$, where T is the period. This fact, in view of (10), implies the second statement. □

Remark 2. By re-parameterizing θ by φ instead of time t, it is easy to show that $\Lambda(\varphi) = \frac{\partial\theta(\varphi, p_\theta)}{\partial p_\theta}$, which is the conjugate times equation obtained in [10] and analyzed in [2].

E. Conjugate locus of the Serret-Andoyer metric

The extremals of the metric g_a are shown in Fig. 2, where $h = \frac{1}{2}$ and $p_\theta \in [0, \sqrt{I_1}]$: the thick dashed curves correspond to permanent rotations around the minor axis of inertia, and the thick continuous curves to the separating polhoded. Note that physically meaningful solutions of the Euler-Poinsot problem concern $|p_\theta| \in [\sqrt{I_3}, \sqrt{I_1}]$ (trajectories comprises between thick dashed curves). The Gauss curvature is positive in the gray stripe along the horizontal axis. It changes sign along rotational trajectories, while it is positive along oscillating trajectories that remain sufficiently close to the horizontal axis. Such trajectories correspond to the polhodes around the major axis of the energy ellipsoid.

In view of Proposition 2, $\mu(\varphi) \in [A, B]$. The metric g_a is invariant with respect to rotations by angle θ, it possesses the reflectional symmetry induced by $\mu(-\varphi) = \mu(\varphi)$, and $\mu'(\varphi) \neq 0$ for $\varphi \in (0, K(k)\alpha^{-1})$. In particular, ($A_1$), ($A_2$) are both verified. Putting the expression for $\mu(\varphi)$ into (11), we can obtain the exhaustive description of the conjugate locus. We refer to our recent paper [3] for the technical details and present directly the result, illustrated in Fig. 3:

Theorem 1. *The first conjugate locus to a point $(0, \varphi_0)$ of the Serret-Andoyer metric g_a is formed by the conjugate points along oscillating trajectories only. It consists of two components, symmetric with respect to the vertical line $\theta = 0$. Each component of the locus is formed by two smooth branches, which asymptotically tend to the horizontal lines $\varphi = \pm\frac{K(k)}{\alpha}$, and form a unique horizontal cusp on the line $\varphi = -\varphi_0$.*

Denote now by $(\varphi_*(\cdot;\varphi_0), \theta_*(\cdot;\varphi_0))$ a smooth parametrization of the conjugate locus to the point (φ_0, θ_0). Then the classical Poincaré result ([9]) on the minimal distance to the conugate locus implies that along arc-length parametrized geodesics ($h = 1/2$)

$$\min_{\varphi_0} \theta_*(\varphi_0) = \theta_*(0) = \frac{\pi A\sqrt{A}}{\sqrt{(B-A)(C-A)}}.$$

III. Optimal control model of a system of three coupled spin-1/2 particles

A. Problem statement

In [11] and [12] the authors proposed the mehod that reduces the minimal time optimal control problem for a system of three spin-1/2 particles with unequal Ising couplings to the sub-Riemannian problem on $SO(3)$:

$$\dot R(t) = R(t)\begin{pmatrix} 0 & -u_3 & 0 \\ u_3 & 0 & -u_1 \\ 0 & u_1 & 0 \end{pmatrix}, \quad \int_0^T u_1^2 I_1 + u_3^2 I_3 \to \min_{u(\cdot)},$$

where $T > 0$ is fixed. It turns out that this problem can be transformed into an certaint singular Riemannian problem on the sphere S^2. Indeed, denote $r_i = R_{1i}$, then since $\|r\| = 1$, we obtain the metric

$$g = \frac{dr_1^2 + k^2 dr_3^2}{r_2^2}, \quad k^2 = \frac{I_1}{I_3},$$

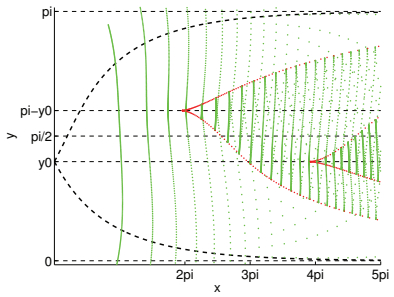

Fig. 3. Right-hand side ($p_\theta > 0$) components of the conjugate locus of Serret-Andoyer metric for $x_0 = 0$, $y_0 = \arccos\sqrt{0.1}$.

having singularity at $r_2 = 0$. In the spherical coordinates $r_1 = \sin\varphi\cos\theta$, $r_2 = \cos\varphi$, $r_3 = \sin\varphi\sin\theta$, the Hamiltonian of this metric takes the form

$$H = \frac{1}{4k^2}\left(p_\varphi^2 + p_\theta^2\cot^2\varphi + \right.$$
$$\left. + (k^2-1)(p_\varphi\cos\theta - p_\theta\cot\varphi\sin\theta)^2\right).$$

Proposition 4. *If $k = 1$, then $H = \frac{1}{4}\left(p_\varphi^2 + p_\theta^2\cot^2\varphi\right)$ defines the standard Grushin metric on S^2.*

Proposition 5. *The family of metrics g depending upon the parameter k have a fixed singularity on the equator $\varphi = \frac{\pi}{2}$ and a discrete symmetry group defined by*

$$H(\varphi, p_\varphi) = H(\pi - \varphi, -p_\varphi), \quad H(\theta, p_\theta) = H(-\theta, -p_\theta).$$

Let us now consider the following two sub-manifolds of $SO(3)$:

$$M_0 = \{R \in SO(3)\ ;\ R^t = (r(0), \cdot, \cdot),\ r(0) = (1,0,0)\},$$
$$M_1 = \{R \in SO(3)\ ;\ R^t = (r(T), \cdot, \cdot),\ r(T) = (0,0,1)\}.$$

Denoting $M^\perp$ the symplectic lift of a sub-manifold $M \in SO(3)$, one can prove the following result:

Proposition 6. *The extremals of the Riemannian metric g on S^2 with boundary conditions $r(0)$, $r(T)$ are extremals of the sub-Riemannian problem on $SO(3)$ with parameter $k^2 = I_1/I_3$, satisfying the boundary conditions $(R(0), \lambda(0)) \in M_0^\perp$, $(R(T), \lambda(T)) \in M_1^\perp$, where λ denotes the adjoint vector.*

This identification allows to parametrize the extremal on $SO(3)$ directly. The Hamiltonian takes the form

$$H_n = \frac{1}{4}\left(\frac{H_1^2}{I_1} + \frac{H_3^2}{I_3}\right).$$

Setting $\cos\vartheta = \frac{H_1}{2\sqrt{I_1}}$, $\sin\vartheta = \frac{H_3}{2\sqrt{I_3}}$, we get

$$\frac{d^2\vartheta}{dt^2} = \frac{\sin 2\vartheta(k^2-1)}{2I_1}, \qquad k^2 = \frac{I_1}{I_3},$$

in which we recognize the pendulum equation. To complete the integration, one can use a suitable parametrization of $SO(3)$, for instance, Euler's angles. Another method is to let $I_2 \to \infty$ in the formulae describing the extremal solutions of the rigid body.

B. Evolution of the conjugate loci: numerical results

We now present the results of numerical computations of conjugate loci of the spin problem using the HamPath code [5]. The initial conditions were taken at $\varphi(0) = \pi/2$, $\theta(0) = 0$, and the evolution of the locus is represented via the deformation of the parameter k starting from $k = 1$. There are two different cases to be analyzed: $k > 1$ and $k < 1$. Since we start from the axis of symmetry, the Hamiltonian $h = p_\varphi^2/4$ at $t = 0$. Restricting the extremals to $h = 1$, we can parameterize he geodesics by $p_\varphi = \pm 2$, $p_\theta \in \mathbb{R}$. By symmetry, we can fix $p_\varphi = -2$ and consider $p_\theta \geq 0$. For any k, the conjugate locus has a contact of order two at the initial point, as $p_\theta \to \infty$.

1) Fig. 4: $k \geq 1$: Observe that θ is not monotonous for all the trajectories. This is true even for small k, like $k = 1.01$, taking $p_\theta = 0.1$ and $T > 14$. Denote $t_*^1(p_\theta, k)$ the first conjugate time and $q_*^1(p_\theta, k) = (\theta_*, \varphi_*)$ the corresponding conjugate point. In Fig. 4.a), we represent the map $k \in [1, 1.5] \mapsto q_*^1(k)$ for $p_\theta = 10^{-4}$. Observe that $\theta(t_*^1(k))$ switches between 0 and π three times at $1 < k_1 < k_2 < k_3 < 1.5$, and $k_2 - k_1 \neq k_3 - k_2$. We then restrict our analysis to $k \leq k_3$.

The subplots b).-d). of Fig. 4 show the deformation of one branch ($p_\varphi = -2$ and $p_\theta \geq 0$) of the conjugate locus for k in $[1, k_1]$, $[k_1, k_2]$ and $[k_2, k_3]$ respectively. For any $k \in [1, k_3]$, the branch is located in the half-plane $\theta \geq 0$. If we denote by $\bar{k}$, $k_1 < \bar{k} < k_2$, the parameter value such that $\varphi(t_1(\bar{k})) = \pi/2$, then $\bar{k} \approx 1.155$ and the branch form a loop for $\bar{k} \leq k \leq k_3$. The different character of the deformation of the conjugate locus can be seen also analyzing the behavior of the trajectories. For $k \leq k_3$ and $p_\theta \geq 0$ we detected four types of trajectories represented in Fig. 5.

2) Fig. 6: $k \leq 1$: This case is easier to interpret. We give on Fig. 6 the conjugate locus for $k \in \{0.8, 0.5, 0.2, 0.1\}$ with 15 chosen trajectories. The key point is the non-monotony of the θ-variable for $k < 1$.

We conclude this section by Fig. 7 showing the deformation of the conjugate locus on the sphere[1]. Observe that the cusp moves along the meridian with respect to the parameter k. It does not cross the equator for $k < 1$ while for $k > 1$ it first crosses the North pole ($k = k_1$), then the equator ($k = \bar{k}$). For $k \geq \bar{k}$, the conjugate locus has self-intersections. Then, it crosses poles again for $k = k_2$ and k_3. This is repeated for greater values of k making the loops smaller and smaller.

IV. Conclusion

We presented here two 2D models, intrinsically related to the Euler-Poinsot rigid body motion. The new theoretical result of this paper is the explicit construction of the basis of Jacobi vector fields for Darboux-type metrics on 2D surfaces of revolution. The consequences of this computation go beyond the content of this paper. From one hand, it gives an alternative and simplified proof of the conjugate locus equation that we used to describe the structure of the conjugate locus of the Serret-Andoyer metric. On the other hand, even if this result gives no information on the conjugate

[1] only the half $p_\varphi(0) = -2$, $p_\theta(0) \in \mathbf{R}$ is plotted to clarify the figures

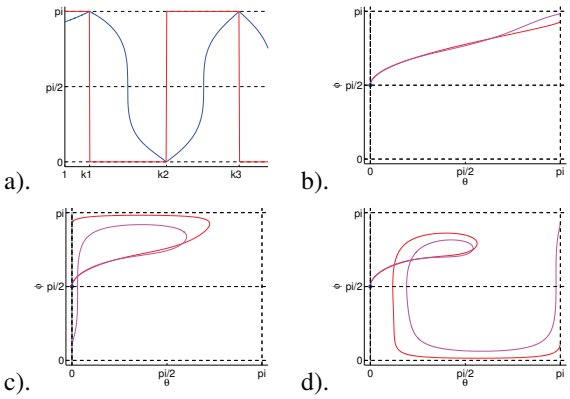

Fig. 4. a). Evolution of q^1_* with respect to k, $p_\theta = 10^{-4}$. In red: $\theta(t^1_*(p_\theta,k))$, in blue: $\varphi(t^1_*(p_\theta,k))$, $k_1 \approx 1.061$, $k_2 \approx 1.250$, $k_3 \approx 1.429$. Figures b).- d).: the deformation of one branch ($p_\varphi = -2$ and $p_\theta \geq 0$) of the conjugate locus w.r.t. the parameter $k \in [1,k_3]$: (b) $k = 1.0, 1.05$; (c) $k = 1.1, 1.2$; (d) $k = 1.3, 1.4$.

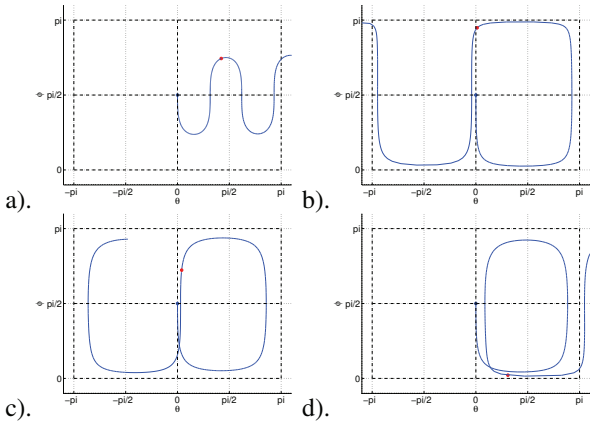

Fig. 5. The four types of trajectories which clarify the evolution of the conjugate locus. a). $1 \leq k \leq k_3$: the only type with monotone non-decreasing $\theta \in [0,t^1_*]$; b). $k_1 \leq k \leq k_3$. c). $\bar{k} \leq k \leq k_3$; d). $k_2 \leq k \leq k_3$.

locus of the original 3D problem since the Serret-Adoyer transformation mixes the state and the co-state variables, it can be used to describe the dynamics of the Jacobi fields basis in of the Euler-Poinsot problem in 3D.

The numerical results on spin dynamics, presented in Section III, significantly improve the results of [12]. They also give an idea about the complexity of the conjugate locus of the Euler-Poinsot problem in 3D, since this problem can be seen as a limit case $I_2 \to \infty$.

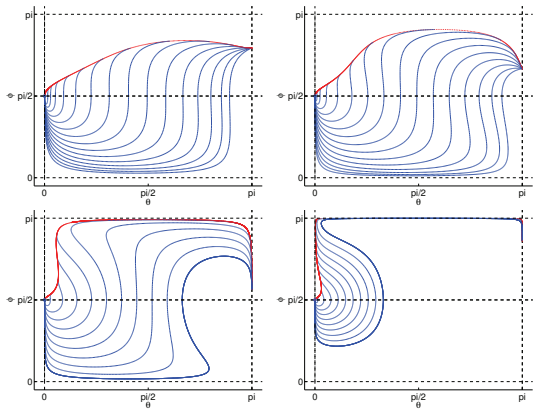

Fig. 6. Conjugate locus with 15 trajectories for $k = 0.8, 0.5, 0.2, 0.1$ from top left to bottom right.

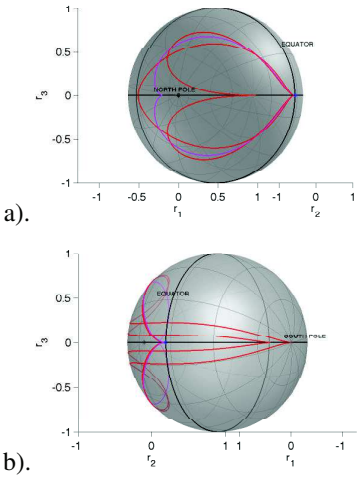

Fig. 7. Conjugate locus on the sphere, magenta curve: $k = 1$ (Grushin metric). a). red curves: $k = 0.8$, 1.15; b). red curves $k = 1.2$, 1.25.

REFERENCES

[1] V.I. Arnold, Mathematical methods of classical mechanics, 2 ed., Graduate texts in Mathematics, 60. Springer-Verlag, New York, 1989.

[2] B. Bonnard, J.-B. Caillau, R. Sinclair, M. Tanaka. Conjugate and cut loci of a two-sphere of revolution with application to optimal control. Ann. Inst. H. Poincaré Anal. Non Linéaire 26 (2009), no. 4, pp. 1081-1098.

[3] B. Bonnard, O. Cots, J.-B. Pomet, N. Shcherbakova. Riemannian metrics on 2D manifolds related to the Euler-Poinsot rigid body problem, 2012, submitted;

[4] P. Gurfil, A. Elipe, W. Tangren, M. Efroimsky, The Serret-Andoyer formalism in rigid-body dynamics. I. Symmetries and perturbations. Reg. Chaotic Dyn. 12 (2007), no. 4, pp. 389-425.

[5] http://cots.perso.math.cnrs.fr/hampath/

[6] V. Jurdjevic, Geometric control theory, Cambridge Studies in Advanced Mathematics, Cambridge University Press, Cambridge, 1997.

[7] M. Lara, S. Ferrer, Integration of the Euler-Poinsot Problem in New Variables, submitted to Mechanics Research Communications, 2010.

[8] K. Y. Lum, A.M. Bloch. Generalized Serret-Andoyer transformation and applications for the controlled rigid body. Dynamics and Control (1999), Vol.9 no. 1, pp.39-66.

[9] H. Poincaré. Sur les lignes géodésiques des surfaces convexes. Trans. Amer. Math. Soc., 1905, 6, pp. 237-274.

[10] K. Shiohama, T. Shioya, M. Tanaka, The geometry of total curvature on complete open surfaces, Cambridge Tracts in Mathematics, 159. Cambridge University Press, Cambridge, 2003.

[11] H. Yuan. Geometry, optimal control and quantum computing. Phd Thesis, Harvard, 2006.

[12] H. Yuan, R. Zeier, N. Khaneja, S. Lloyd. Elliptic functions and efficient control of Ising spin chains with unequal couplings. Ph. Rev. A 77, 032340, 2008.